J. King Saud Univ., Vol. 7, *Eng. Sci.* (2), pp. 219–246 (A.H. 1415/1995)

MECHANICAL ENGINEERING

Two-dimensional Heat Conduction in a Composite Slab with Temperature-Dependent Conductivity

Sami A. Al-Sanea

Mechanical Engineering Department, College of Engineering, King Saud University, P.O. Box 800, Riyadh 11421, Saudi Arabia

(Received 27/10/1993; Accepted for publication 28/2/1994)

Abstract. A numerical model, based on the finite-volume method, is developed and applied for the determination of the two-dimensional, steady-state temperature variation in a composite slab with temperature-dependent thermal conductivity. Results of application to four cases are compared in which the slab can be: (1) homogeneous with constant conductivity, (2) composite with temperature-independent conductivity, (3) composite with linear temperature-dependent conductivity, and (4) composite with non-linear temperature-dependent conductivity. Analytical solutions are utilized for the first three cases and show excellent agreement with the numerical results. A parametric study is carried out to investigate the effects of grid size, conductivity ratio of materials in the composite and various forms of conductivity-temperature relations. The temperature distribution is found to remain unaltered to change in conductivity for a conductivity ratio greater than about 100. The superiority of using the harmonic mean of the nodal-face conductivity is demonstrated.

Nomenclature

A,B,C	=	finite-difference coefficients
IX1&2	=	grid indices for locating interface
k	=	thermal conductivity defined by Eq. (5)
k_{ref}	=	reference conductivity
K	=	dimensionless conductivity, k/k_{ref}
l	=	length of slab
n	=	temperature exponent used in Eq. (5)
NI,NJ	=	number of nodes in x and y directions, respectively
T	=	temperature

TOLER = tolerance for normalized total residual error
U = transformed temperature defined by Eq. (7)
ω = width of slab
x,y = coordinate directions
x_i = interface location
X,Y = dimensionless coordinates, x/*l*, y/*l*, respectively

Greek symbols

α = under-relaxation factor
β = temperature coefficient used in Eq. (5)
γ = thermal conductivity ratio, $k_{1,o}/k_{2,o}$
δx, δy = inter-nodal distances, Fig. 2
θ = dimensionless temperature, $(T-T_b)/(T_l-T_b)$

Subscripts

b,*l*,r = bottom, left and right boundaries, respectively
e,n,s,w = relate to nodal faces, Fig. 2
E,N,P,S,W = finite-difference grid points
m,1,2 = m = 1 for material 1, m = 2 for material 2
o = reference value

Introduction

The problem considered and practical relevance

In many heat-transfer applications, the heat-conduction medium is composed of multiple layers of materials with different thermal properties. Examples are found in furnaces and ovens, electronic components, thermal insulation systems and in composite fins. The cooling and heating loads of buildings depend on the thermal behavior in the composite constructions of their walls and roofs. Roads and highways are constructed using an asphalt-concrete composite with the soil layer beneath; temperature variations and thermal stresses are of major interest to the engineer who is concerned with the cracks forming under different traffic-load conditions. It is, therefore, important to be able to calculate the temperature distribution and heat-transfer rate in composite structures under different boundary conditions and material properties. The thermal conductivity of materials varies with temperature in different ways; for most pure metals it decreases with increasing temperature, whereas for most insulating materials it increases with temperature. When small temperature differences are involved, the conductivity can be approximated to vary linearly with temperature; in general, however, the relation is nonlinear. These forms of temper-

ature dependence, which must be accounted for in the analysis, give rise to nonlinear conditions. Materials in which the thermal conductivity depends upon the direction of heat flow, anisotropic materials, are not addressed in the present study.

Review of previous work

One-dimensional studies

Ozisik [1] described various methods for solving one-dimensional, time-dependent heat conduction in composite media with temperature independent properties. Such methods include the separation of variables, Green's function, Laplace and integral transforms. The Laplace transform was used with various boundary conditions [2-5]. Periodic boundary conditions were applied by Han [6] in a semi-analytic approach using complex algebra. Radiative boundary conditions were applied by Sunden [7] in a finite-difference solution. Hagen [8] used a linear perturbation series with a spatially-dependent conductivity.

Nonlinear, one-dimensional, time-dependent heat conduction in a homogeneous medium was studied by [1; 9-13] amongst many. The studies dealt mainly with a linear temperature-dependent thermal conductivity. The method of successive approximation was used by Yang [9] in a semi-infinite solid; Halle [10] solved a similar problem by applying the Kirchhoff transformation. A perturbation method was employed by Aziz and Na [11] in analyzing the periodic heat transfer in fins; a similar technique was used by Jones [12] in a slab with temperature dependent heat generation. Kar *et al.* [13] presented analytical and numerical solutions by applying the Kirchhoff transformation and the method of characteristics.

Multi-dimensional studies

Multi-dimensional heat conduction problems in composites with temperature-independent properties were studied by, for example, [14-20]. Huang and Chang [14] used the Green's functions and incorporated a linear temperature-dependent heat generation in laminated composites. Palisoc *et al.* [15] presented a solution in the form of a double Fourier integration. The finite-element method was used by Tamma and Yurko [16]. Thermal analyses of straight composite fins were carried out [17-19]. Mikhailov and Ozisik [20] used the separation of variables and split up the multi-dimensional problem into 1-D eigenvalue problems.

Variable thermal conductivity in multi-dimensional heat conduction problems were investigated by, for example, [21-24]. The studies dealt with a linear temperature-dependent conductivity in homogeneous [21-23] and in composite [24] media.

Campo [21] presented a quasi-analytical procedure based on a regression analysis, while Wrobel [22] presented a boundary element method and used the Kirchhoff transformation and an iterative Newton-Raphson technique. The finite-difference method was employed by Zhao *et al.* [23]. Chang and Payne [24] developed an exact solution in a two-material-layer slab using the Kirchhoff transformation and the method of separation of variables.

In summary, it is concluded from the above review that investigations of multi-dimensional problems in composites with temperature-dependent properties are scarce. Besides, analytical solutions to this class of problems are limited to linear temperature-dependent properties and to simple configurations and boundary conditions.

Objectives of the present work

The main objectives of this work are to develop a numerical model and conduct a study of two-dimensional, steady-state heat conduction in a composite structure with temperature-dependent conductivity. The rectangular configuration depicted in Fig. 1 is considered in which analytical solutions, under simplified conditions, are available for comparison. The model is applied to four slab cases: (1) homogeneous with constant conductivity, (2) composite with temperature-independent conductivity, (3) composite with linear temperature-dependent conductivity, and (4) composite with nonlinear temperature-dependent conductivity.

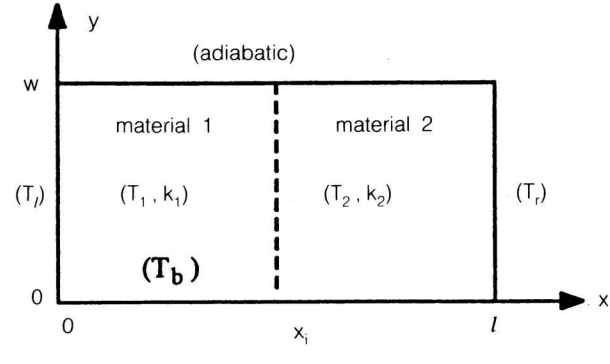

Fig. 1. The composite slab configuration

Mathematical Formulation

Basic assumptions

In order to keep the problem relatively simple so that closed form analytical solutions can be developed for validating the numerical model, the following assumptions are made. Steady-state and two-dimensional conditions are considered in an isotropic two-layered slab with no heat generation. Perfect thermal contact is assumed at the interface. The thermal conductivity of either material can vary with temperature.

It is worth noting that the thermal contact resistance may be substantial in some cases. This depends upon empirical information and factors such as: the materials involved, the surface conditions, the binder, the interface temperature, and the pressure exerted on the composite. Therefore, the present analysis may only be used to address such practical problems in an idealized manner.

The governing equations

Based on the above assumptions, the equation governing the heat conduction in the composite is given for materials 1 and 2 by:

$$\frac{\partial}{\partial x}\left(k_m \frac{\partial T_m}{\partial x}\right) + \frac{\partial}{\partial y}\left(k_m \frac{\partial T_m}{\partial y}\right) = 0 \tag{1}$$

where the subscript $m = 1$ relates to material 1 bounded by $0 < x < x_i$ and $0 < y < \omega$, and $m = 2$ relates to material 2 bounded by $x_i < x < l$ and $0 < y < \omega$.

By defining appropriate dimensionless parameters, as given in the nomenclature, Eq. (1) is cast in a nondimensional form as:

$$\frac{\partial}{\partial X}\left(K_m \frac{\partial \theta_m}{\partial X}\right) + \frac{\partial}{\partial Y}\left(K_m \frac{\partial \theta_m}{\partial Y}\right) = 0 \tag{2}$$

Boundary conditions

The composite top boundary is taken to be adiabatic while the other boundaries are isothermal with temperatures as given in Fig. 1 and described in a dimensionless form by:

$$\theta = 1 \qquad \text{at } X = 0 \text{ and } 0 < Y < \omega/l,$$

$$\theta = \theta_r \qquad \text{at } X = 1 \text{ and } 0 < Y < \omega/l,$$

$$\theta = 0 \qquad \text{at } Y = 0 \text{ and } 0 < X < 1, \text{ and}$$

$$\partial\theta/\partial Y = 0 \qquad \text{at } Y = \omega/l \text{ and } 0 < X < 1. \tag{3}$$

The conditions at the interface ($X = x_i/l$) are:

$$\theta_1 = \theta_2,$$

$$K_1 (\partial\theta_1/\partial X) = K_2 (\partial\theta_2/\partial X). \tag{4}$$

Thermal-conductivity-temperature relations

The conductivity (k_m) varies with temperature (θ) according to:

$$k_m = k_{m,o} (1 + \beta_m \theta^{n_m}), \tag{5}$$

where $k_{m,o}$ is the thermal conductivity of material m at the reference temperature of $\theta = 0$. Appropriate values of the coefficient β_m and the exponent n_m can represent the conductivity-temperature dependence of many practical materials.

Analytical solutions

Case 1: Homogeneous slab with constant k

With reference to Eq. (5), this case corresponds to $k_1 = k_2$ and $\beta_m = 0$. The governing equation becomes linear and its solution, under the nonhomogeneous boundary conditions given by Eq. (3), is obtained by the separation of variables method and the principle of superposition as:

$$\theta(X,Y) = [T(X,Y) - T_b)/(T_t - T_b)],$$

$$T(X,Y) = \frac{4}{\pi}\sum_{n=1}^{\infty} \frac{\sin(\lambda_n l Y)}{n \sinh(\lambda_n l)} [T_t \sinh\{\lambda_n l(1-X)\} + T_r \sinh(\lambda_n l X)], \tag{6}$$

where the eigenvalues are: $\lambda_n = n\pi/2\omega$ for n = 1,3,5, ...

Case 2: Composite slab with k independent of θ

This case corresponds to $k_1 \neq k_2$ and $\beta_m = 0$, see Eq. (5). Equations (1) to (4) were solved analytically for T_1 and T_2 by using the method of separation of variables, Chang and Payne [24].

Case 3: Composite slab with linear k(θ)

This case corresponds to $n_m = 1$ in which a linear relation between k_m and θ exists for finite values of β_m. The governing equation becomes nonlinear and Eqs. (1) to (4) were solved analytically for $U_1(x,y)$ and $U_2(x,y)$ by Chang and Payne [24] using the Kirchhoff transformation and the method of separation of variables. The values U_1 and U_2 are the transformed temperatures T_1 and T_2 given by:

$$U_m = \int_{T_{m,o}}^{T_m} \frac{k_m(T)}{k_{m,o}}\, dT, \tag{7}$$

where $T_{m,o}$ is a reference temperature and $k_{m,o}$ is the value of $k_m(T)$ at $T_{m,o}$. Substituting Eq. (5), with $n_m = 1$, into Eq. (7) and taking $T_{m,o}$ to be zero, one gets after integration:

$$T_m(x,y) = \frac{1}{\beta_m}\left[\left\{1 + 2\beta_m U_m(x,y)\right\}^{1/2} - 1\right] \tag{8}$$

In the present study, the analytical equations derived by Chang and Payne [24] for U_m are used in conjunction with Eq. (8) to obtain $T_m(x,y)$ for comparison with the numerical results.

Case 4: Composite slab with nonlinear k(θ)

When n_m is not equal to unity, a nonlinear relation between k_m and θ exists for finite values of β_m, see Eq. (5), and closed form analytical solutions are not possible.

Numerical Solution Procedure

Introduction

The numerical solution procedure is based on the finite-volume method. The essence of the procedure is to replace the governing partial-differential equation (1) by a set of finite-difference equations (f.d.e.'s) and to provide a method for their sol-

ution. Use is made of the computer program TEACH-C, Gosman, *et al.* [25], which is modified for the present problem. The following sections give the salient features of the procedure; for more details, see [25].

The finite-difference grid

The physical domain is discretized into a number of control volumes (cells) by imposing a rectilinear grid composed of coordinate lines. The temperature and thermal conductivity are calculated and stored at the discrete points formed by the grid-line intersections (nodes). The grid need not be uniform and, hence, nodal points can be concentrated in regions where temperature gradients are steep. This enhances the accuracy and economy of the method. A representative portion of the grid is depicted in Fig. 2 which shows a typical node P and its neighbours N,S,E and W, together with various items of notations. The intervening control volume boundaries are denoted by lower-case version of the same letters, n,s,e and w.

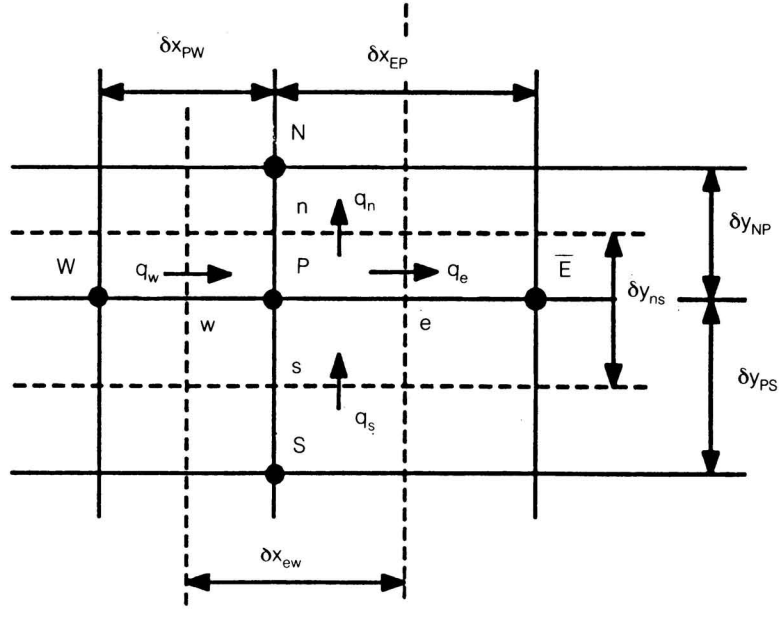

Fig. 2. A typical cluster of grid nodes and associated notation

The finite-difference equations

A finite-difference equation counterpart of the differential equation (1) is derived for the representative node P shown in Fig. 2. Equation (1) is integrated over

the control volume surrounding P as follows (the subscript m is removed for clarity):

$$\int_s^n \int_w^e \left[\frac{\partial}{\partial x}\left(k \frac{\partial T}{\partial x} \right) + \frac{\partial}{\partial y}\left(k \frac{\partial T}{\partial y} \right) \right] dx \; dy = 0 \tag{9}$$

(i) *The integrated conduction terms in the x-direction* (I_1):

$$\begin{aligned} I_1 &= [k\, \delta y_{ns}\, \partial T/\partial x]_e - [k\, \delta y_{ns}\, \partial T/\partial x]_w \\ &= k_e\, \delta y_{ns}\, (T_E - T_P)/\delta x_{EP} - k_w\, \delta y_{ns}\, (T_P - T_W)/\delta x_{PW} \\ &= A_E (T_E - T_P) + A_W (T_W - T_P), \end{aligned} \tag{10}$$

where

$$A_E = k_e\, \delta y_{ns}/\delta x_{EP} \quad \text{and} \quad A_W = k_w\, \delta y_{ns}/\delta x_{PW}. \tag{11}$$

(ii) *The integrated conduction term in the y-direction* (I_2):

$$\begin{aligned} I_2 &= [k\, \delta x_{ew}\, \partial T/\partial y]_n - [k\, \delta x_{ew}\, \partial T/\partial y]_s \\ &= A_N (T_N - T_P) + A_S (T_S - T_P), \end{aligned} \tag{12}$$

where

$$A_N = k_n\, \delta x_{ew}/\delta y_{NP} \quad \text{and} \quad A_s = k_s\, \delta x_{ew}/\delta y_{PS}. \tag{13}$$

Assembly of terms I_1 and I_2 yields:

$$A_N(T_P - T_N) + A_S (T_P - T_S) + A_E (T_P - T_E) + A_W (T_P - T_W) = 0,$$

or

$$\sum_{i}^{N,S,E,W} A_i (T_p - T_i) = 0. \tag{14}$$

Equations (14) are the finite-difference (volume) energy conservation equations. These equations are nonlinear since their coefficients, given by Eqs. (11) and (13), depend on the temperature itself, through the conductivity. The nonlinearity is handled within the framework of the iterative procedure described briefly in the next Section. The nodal-face conductivities k_n, k_s, k_e and k_w are evaluated by the harmonic mean of the nodal values; more details are given later. The boundary conditions are incorporated through appropriate adjustments to the f.d.e.'s of the boundary nodes. Equations (14) are written, one for each node; the outcome is a set of simultaneous algebraic equations whose number equals that of the unknown temperatures. The task now is to solve these simultaneous equations.

Solution of the finite-difference equations

Equations (14) are recast into the following form:

$$(A_P - B_P)\, T_P = \sum_{i}^{N,S,E,W} A_i\, T_i + C_P \tag{15}$$

where $A_P = \sum_i^{N,S,E,W} A_i$, B_P and C_P are used to introduce the boundary conditions into the boundary nodes; for interior nodes, B_P and C_P are zero.

The solution of the set of Eqs (15), for all unknown nodal temperatures, is achieved by an iterative Line-by-Line procedure combined with a Block-Adjustment enhancement. The Line procedure involves the simultaneous solution for the temperature, along each grid line, by a particular form of Gaussian elimination which is the well known "Thomas Algorithm" or "Tri-Diagonal Matrix Algorithm (TDMA)". The Block-Adjustment procedure is applied to enhance the rate of convergence of the iterative steps. Its essential feature is to increment the temperatures during the iterative process by values, calculated from an overall energy balance, to satisfy the conservation of energy principle. The values of thermal conductivity are updated within the iterative process, according to Eq. (5), using the latest calculated temperatures.

Evaluation of nodal-face conductivity

When the thermal conductivity varies with temperature or, in general, with location as in composites, the nodal-face conductivity values need to be evaluated from those calculated and stored at the nodal points. The nodal-face conductivities, k_n, k_s, k_e and k_w, are used in calculating the heat-transfer rates at the control-volume (cell) faces, which lie midway between grid points, and are contained in the finite-dif-

ference coefficients given by Eqs (11) and (13). Consider, for example, the east face of the nodal point P shown in Fig. 2. A straightforward procedure for obtaining k_e is to assume a linear variation of k between points P and E, hence:

$$k_e = (k_P + k_E)/2 \tag{16}$$

This expression gives the arithmetic mean which is, incidentally, the standard practice used in the TEACH-C code and is sufficient for most situations. However, when the conductivity varies sharply across an interface or when large temperature variations exist, the arithmetic mean is found to be inaccurate; this is demonstrated later in the section "Effects of nodal-face conductivity". Patankar [26;27] proposed the use of a physically more realistic alternative and of a comparable simplicity; namely, the harmonic mean. The expression for k_e, for example, using the harmonic mean is given by, [27]:

$$k_e = 2\, k_P\, k_E / (k_P + k_E). \tag{17}$$

The harmonic mean, thus, replaces the arithmetic mean and is used through the present study.

Stability, convergence and accuracy of the iterative procedure

The stability of the process is procured by the satisfaction of the standard requirement for convergence of an iterative solution method; namely, the diagonal dominance of the coefficient matrix. With reference to the f.d.e.'s, Eqs (15), this requirement is expressed as:

$$| A_p - B_p | \geq \sum_i | A_i | \tag{18}$$

at all grid nodes. The stability criterion is always obeyed when the coefficients B_p are either zero or negative. This criterion is valid for linear equations with constant coefficients; however, it is also valid when the coefficients are 'mild' functions of temperature [25]. For strongly nonlinear problems, it is sometimes necessary to damp the changes in temperature which occur between iterations. This may be achieved by the introduction of an under-relaxation factor α ($0 < \alpha < 1$) and evaluating T_P as:

$$T_P = \alpha\, T_P^N + (1 - \alpha)\, T_P^{N-1}, \tag{19}$$

where T_P^N and T_P^{N-1} are the solutions at the N^{th} and $(N - 1)^{th}$ iterations, respectively.

Under the conditions of the present study, the solutions are found to be stable without the need for an under-relaxation factor.

Convergence

A converged solution is achieved when the changes in temperature, for all nodes, produced by successive iterations diminish and when the sum of the absolute values of residual errors in the f.d.e.'s is reduced to a prescribed small value. The latter may be a specified small fraction of a suitable reference quantity, such as the total heat transfer rate. More details are given in the appendix.

Accuracy

In common with all finite-difference procedures, the accuracy of the present method depends on specifying sufficiently small space intervals. It is, therefore, necessary always to ensure that the solution is invariant to further reduction in these intervals. This is dealt with in Section of "Finite-difference grid independence test".

Other computational details and a typical computer output are given in the appendix.

Results and Discussion

Introduction

The calculations are carried out for the following parameters: $\omega = 1/2$, $x_i = 1/2$, $k_{2,o} = 1$ W/m.K, $\theta_I = 1$, $\theta_r = 0.1$ and $\theta_b = 0$. The thermal conductivity ratio, $\gamma = k_{1,o}/k_{2,o}$, is a variable parameter and is altered by varying $k_{1,o}$.

Finite-difference grid independence test

An investigation is made in order to establish an optimum grid to use. For this purpose, the conditions of Case 2 with $\gamma = 100$ are chosen. The results of four grids are examined and compared with the exact solution. The grid sizes (NI × NJ) are: 8 × 6, 12 × 8, 18 × 12 and 30 × 20. The grid lines are nonuniformly spaced and concentrated in regions of high temperature variations. Figures 3 and 4 show the temperature distributions along the adiabatic boundary (Y = 0.5) and interface (X = 0.5), respectively. Not all the numerical results are displayed for clarity reasons. It is seen that the solutions obtained with the coarse grids exhibit grid dependence, especially at the interface; the solution obtained with the finest grid (30 × 20) is practically grid independent and falls on the exact solution. Further grid refinement is, therefore, unnecessary and the grid of 30 × 20 is used throughout the study.

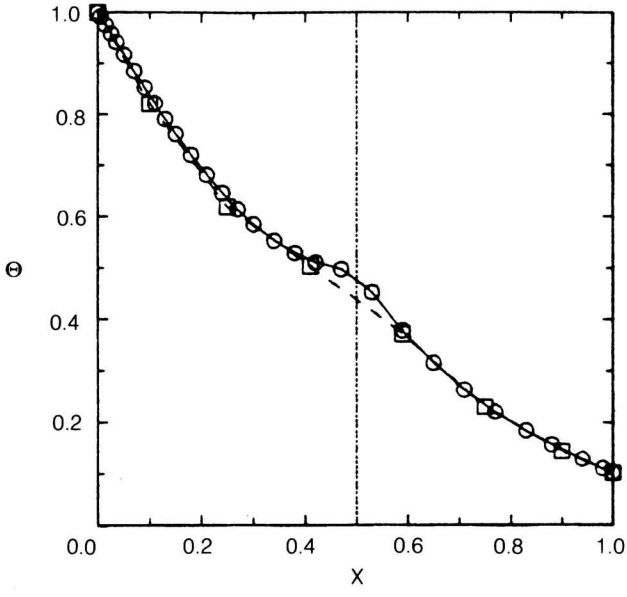

Fig. 3. Temperature variation along adiabatic boundary showing effects of grid size for Case 2, $\gamma = 100$: − □ − NI = 8, NJ = 6; ○ NI = 30, NJ = 20; − exact

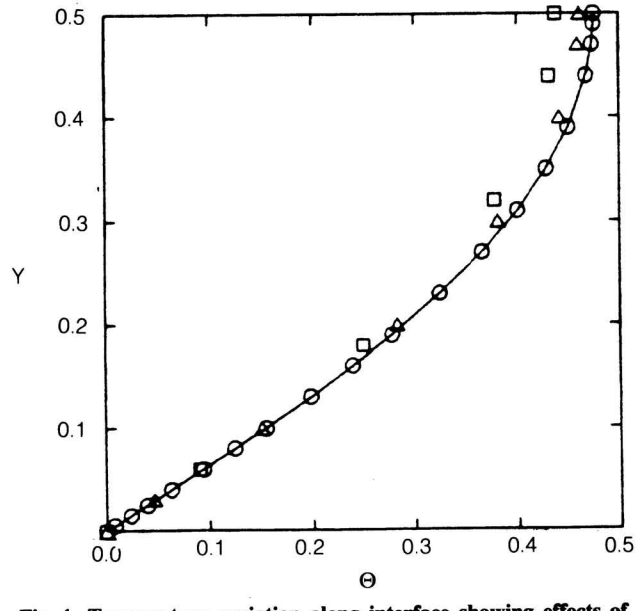

Fig. 4. Temperature variation along interface showing effects of grid size for Case 2, $\gamma = 100$: □ NI = 8, NJ = 6; △ NI = 12, NJ = 8; ○ NI = 30, NJ = 20; − exact.

Case 1: Homogeneous slab with constant k

The pertinent parameter that distinguishes Case 1 is $\gamma = 1$. The results for this case are used for comparison with those of other cases to be presented next.

Case 2: Composite slab with k independent of θ

The dimensionless parameter which characterizes this case is γ. The results showing the effects of different values of γ on the temperature distribution are compared for $\gamma = 10$, 100 and 1000; $\gamma = 1$ relates to the homogeneous slab (Case 1). Figure 5a depicts the temperature variations versus distance (X) along the adiabatic boundary ($Y = 0.5$); the temperature variations versus distance (Y) along the interface ($X = 0.5$) are given in Fig. 5b. The exact solutions are shown as solid lines for comparison. While the temperature for the homogeneous slab ($\gamma = 1$) varies smoothly across the plane at $X = 0.5$, the presence of the interface causes a local discontinuity in the region, as seen in Fig. 5a. This discontinuity arises from the fact that the products of the temperature gradient and the conductivity are equal at the interface, cf. Eq. (4). It should be mentioned, however, that the lines connecting the pair of discrete temperature values on either side of the interface ($X = 0.5$) in Fig. 5a are smeared due to graphical interpolation. The results shown in Figs 5a and 5b indicate that the temperature level increases over the whole slab as γ increases to about 100. This is due to a decrease in thermal resistance of material 1 as a result of increasing conductivity. It is also interesting to note that the temperature values obtained with $\gamma = 100$ and 1000 are practically identical. In other words, when γ is large (*approximately* > 100), the temperature remains unaltered with changing conductivity. This is since the thermal resistance of material 1 becomes relatively very small at which the temperature distribution becomes unaffected by the internal resistance and wholly determined by the conditions imposed along the boundaries. As to the agreement between the numerical and analytical results, this can be described as excellent.

The temperature contours displayed in Figs. 6a to 6d give detailed information about the effects of γ and emphasize the results discussed above. These contours are constructed from the numerical temperatures which are practically the same as the analytical values. Sharp temperature variations are calculated near the bottom left corner; the adiabatic boundary ($Y = 0.5$) is characterized by contour lines that run normal to it. Due to the homogeneity of the slab material for $\gamma = 1$, Fig 6a displays smooth temperature contours over the whole region. The contour lines across the interface ($X = 0.5$) in Figs. 6b to 6d are smeared due to interpolation by the contour graphics package.

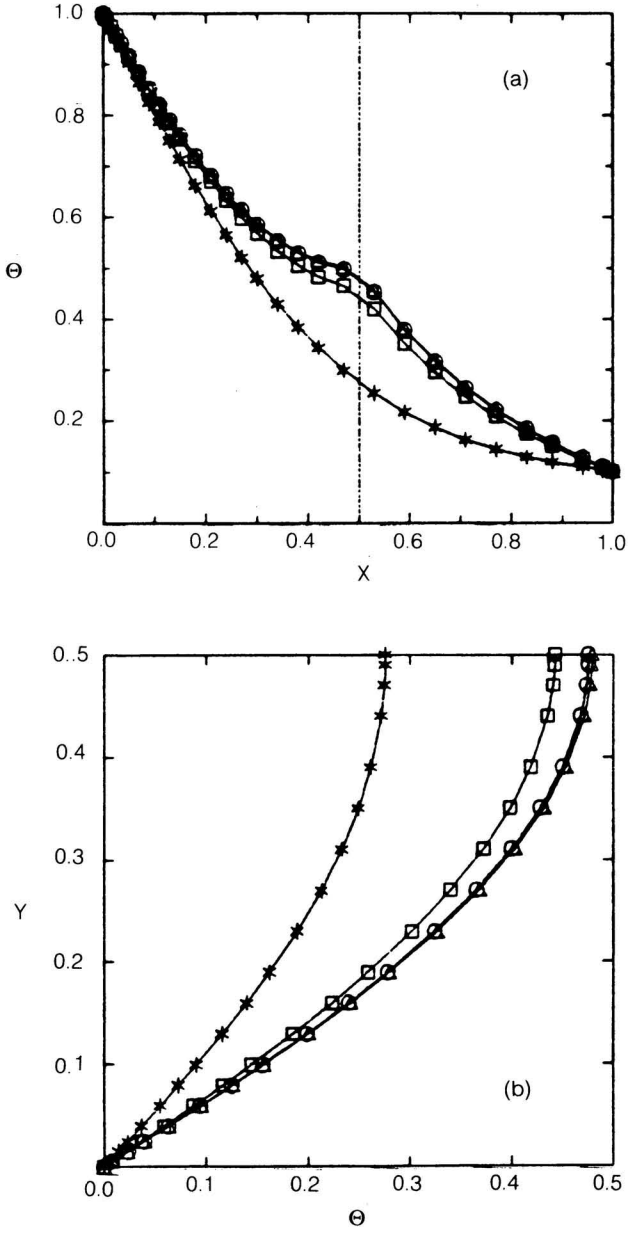

Fig. 5. Temperature variations along adiabatic boundary (a) and interface (b) showing effects of conductivity ratio for Case 2: * $\gamma = 1$, □ $\gamma = 10$, ○ $\gamma = 100$, △ $\gamma = 1000$; (symbols) = numerical, − exact.

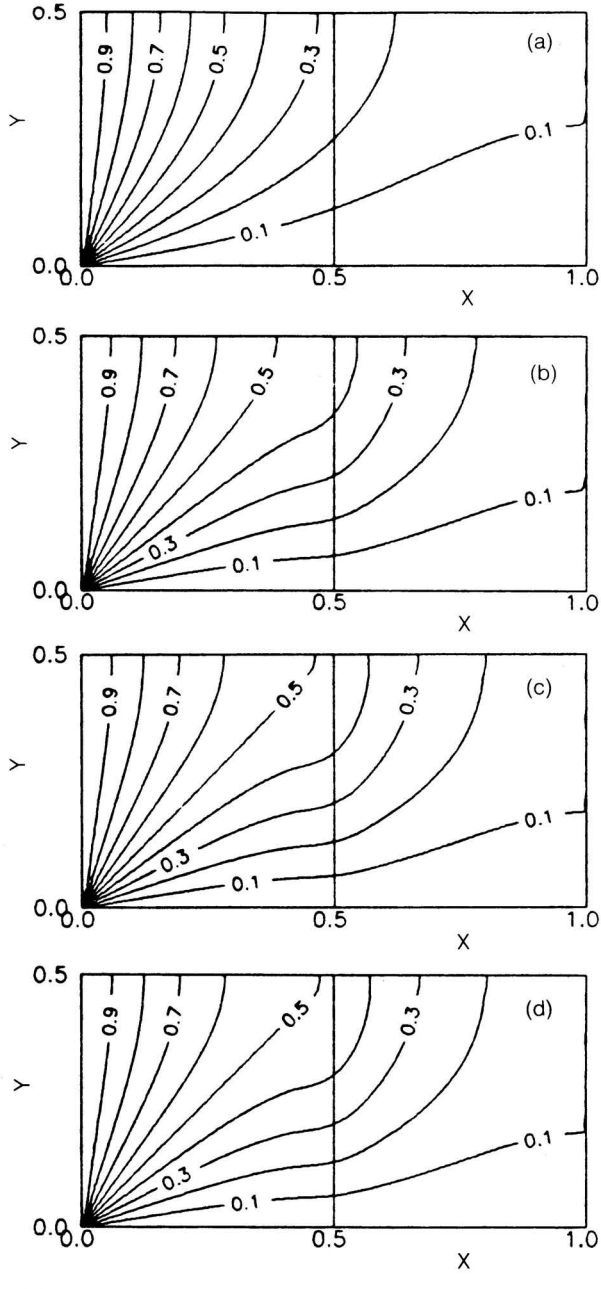

Fig. 6. Temperature contours showing effects of conductivity ratio for temperature-independent conductivity: (a) $\gamma = 1$, (b) $\gamma = 10$,(c) $\gamma = 100$ and (d) $\gamma = 1000$.

Case 3: Composite slab with linear k(θ)

The parameter that characterizes Case 3, besides γ, is β_m, see Eq. (5). The exponent n_m is set to unity in which the conductivity would vary linearly with temperature. The present case is studied for $\gamma = 100$; three different values of the coefficient β_m, which determine the relative dependence of k on θ, are considered, namely, $\beta_1 = \beta_2 = 1$, $\beta_1 = \beta_2 = 2$ and $\beta_1 = \beta_2 = 3$. The results are presented in Figs 7 and 8 and are to be compared with those for $\beta_m = 0$ and $\gamma = 100$ of Case 2. It is seen that the parameter β_m has a noticeable effect on the results; however, the general pattern of temperature distribution remains similar as it is controlled by the boundary conditions of the problem. The temperature level increases over the whole slab with increasing conductivity, due to an increase in β_m. The positive values chosen for β_m relate to materials in which the thermal conductivity increases with temperature. The mathematical model should, equally well, work with negative values of β_m which pertain to materials in which k_m decreases with θ. The agreement between the numerical results and analytical solutions is, once again, excellent.

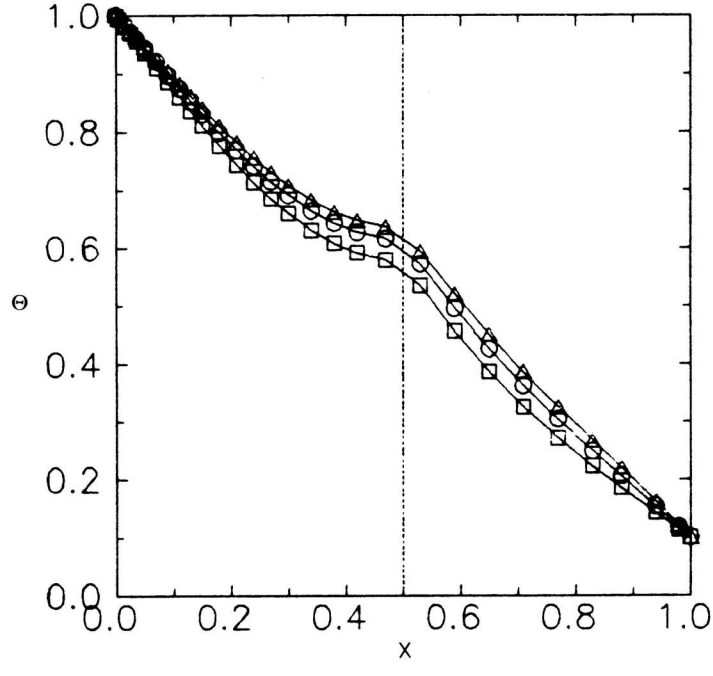

Fig. 7. Temperature variation along adiabatic boundary showing effects of β_m for Case 3, $\gamma = 100$: □ $\beta_1 = \beta_2 = 1$, ○ $\beta_1 = \beta_2 = 2$, △ $\beta_1 = \beta_2 = 3$; (symbols) = numerical, – exact.

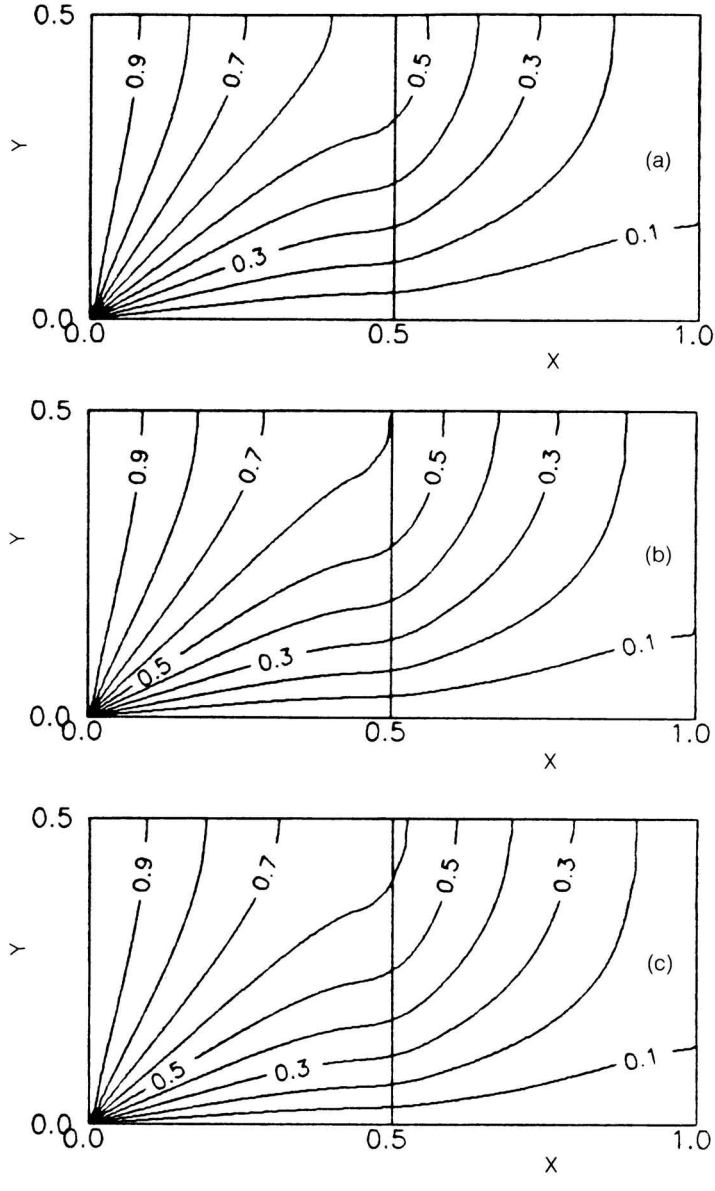

Fig. 8. Temperature contours showing effects of β_m for Case 3, $\gamma = 100$: (a) $\beta_1 = \beta_2 = 1$, (b) $\beta_1 = \beta_2 = 2$ and (c) $\beta_1 = \beta_2 = 3$.

Case 4: Composite slab with nonlinear k(θ)

The extra parameter that characterizes Case 4, besides γ and β_m, is the exponent n_m in the conductivity-temperature relation given by Eq. (5). This case is studied for $\beta_m = 2$ in which the conductivity would vary nonlinearly with temperature for finite values of n_m other than unity. Equation (5) is plotted in Fig. 9 to show the variation of the conductivity, normalized by its reference value, with temperature for $n_m = 0.5$, 2 and 3. The value $n_m = 1$ which gives the linear variation between k and θ (Case 3) is shown for comparison. The results showing the effects of the exponent n_m are presented in Figs 10 and 11 for $\gamma = 100$ and $\beta_m = 2$ and may be compared with those for $n_m = 1$ and $\gamma = 100$ of Case 3. It is seen that the variation in conductivity of material 1 has a more dominant effect on the temperature distribution than that of material 2. This is attributed to the relatively large value of γ. The temperature pattern is similar to before and, hence, warrants no further discussion. However, Case 4 demonstrates the usefulness of the numerical scheme in situations where a closed form analytical solutions are not obtainable.

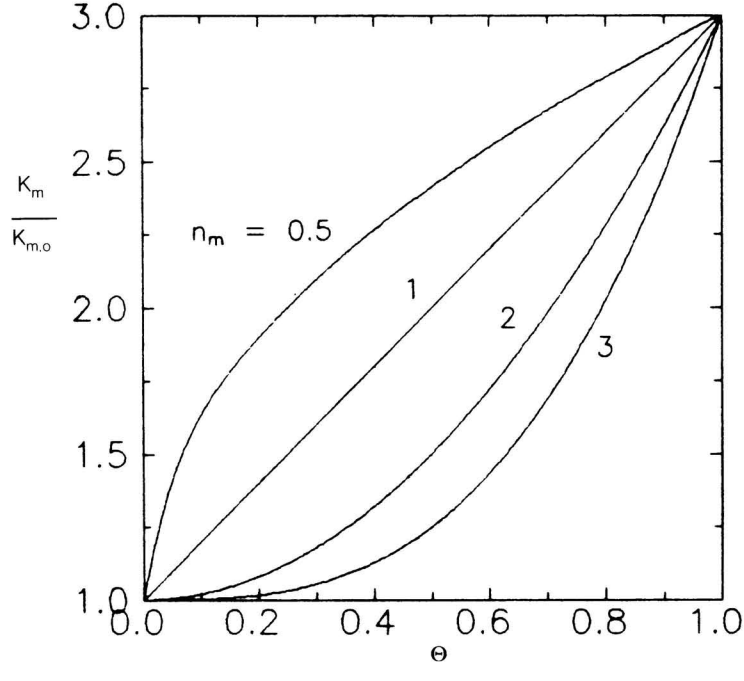

Fig. 9. Normalized conductivity versus temperature according to Eq. (4) for $\beta_m = 2$ and different values of n_m.

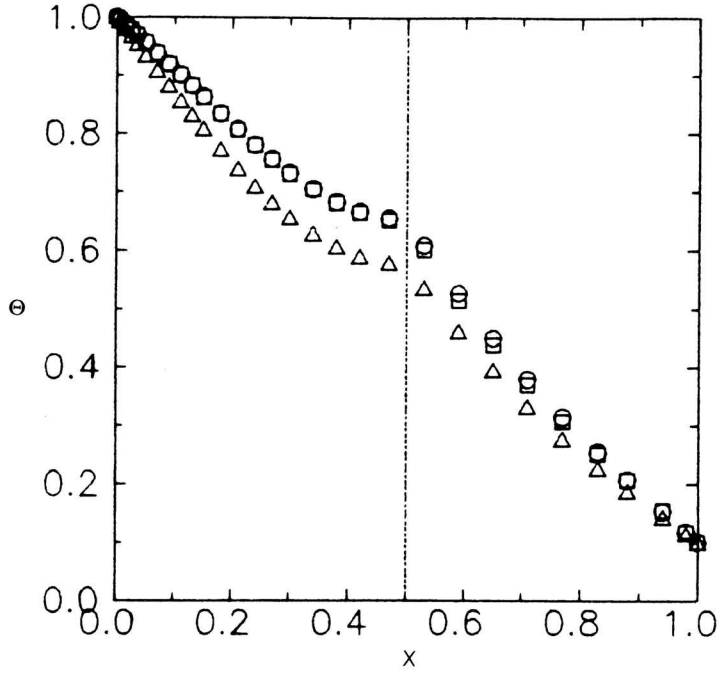

Fig. 10. Temperature variation along adiabatic boundary showing effects of n_m for Case 4, $\gamma = 100$, $\beta_1 = \beta_2 = 2$: △ $n_1 = 0.5$, $n_2 = 2$; □ $n_1 = 3$, $n_2 = 0.5$; ○ $n_1 = 3$, $n_2 = 2$.

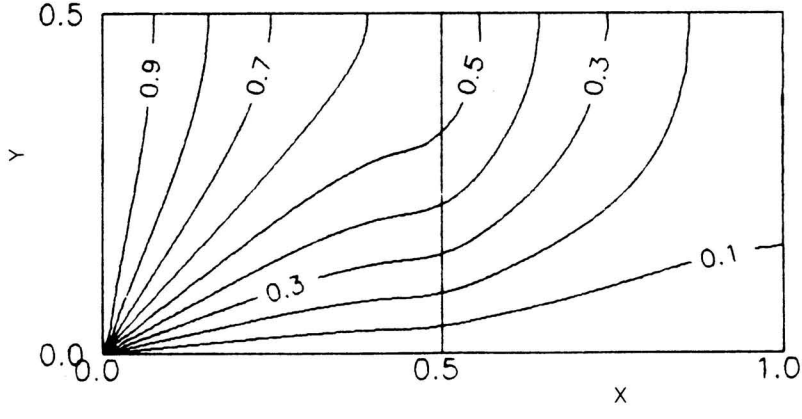

Fig. 11. Temperature contours for Case 4, $\gamma = 100$, $\beta_1 = \beta_2 = 2$, $n_1 = 0.5$, $n_2 = 2$.

Effects of nodal-face conductivity

The superiority of using the harmonic mean for calculating the nodal-face conductivity, as compared to using the arithmetic mean, is demonstrated. Case 3 with $\gamma = 100$ and $\beta_1 = \beta_2 = 2$ is chosen for this purpose, and the two sets of numerical results are compared with the exact solution for accuracy. Typical results are presented in Fig. 12 for the temperature variation along the adiabatic boundary. It is shown that while the harmonic mean gives excellent agreement with the exact solution, the arithmetic mean fails to achieve such accuracy with, perhaps, an unacceptable error. It is interesting to note that the discrepancy is small across material 1 and large across material 2 when the arithmetic mean is used. This is because the temperature variation is more sensitive to the errors generated at the interface in the material of the lower conductivity, *i.e.* material 2. The error in temperature using the arithmetic mean, for this case, ranges from 0.05% to 0.3% across the whole of material 1; and from 2% to 8.5% across material 2. The error using the harmonic mean ranges from 0.02% to 0.04% across material 1 and from 0.1% to 0.2% across material 2. The rela-

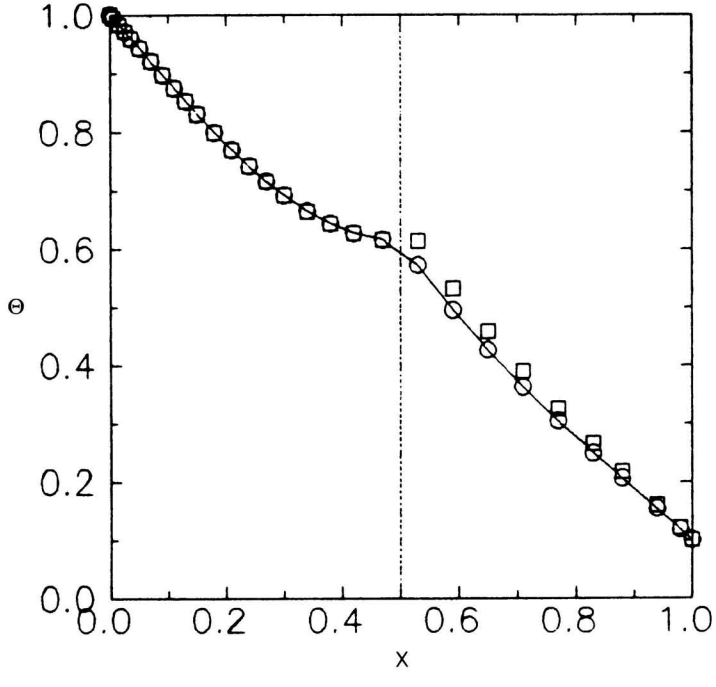

Fig. 12. Temperature variation along adiabatic boundary showing effects of nodal-face conductivity for Case 3, $\gamma = 100$, $\beta_1 = \beta_2 = 2$; ○ harmonic mean, □ arithmetic mean, — exact.

tively large errors that result from the use of the arithmetic mean of nodal-face conductivity can be reduced but at the expense of using much finer finite-difference grids. The cause of such large deviation in the results is due solely to the way in which the nodal-face conductivity is formulated. With reference to Eqs. (16) and (17), it can easily be verified that when the conductivities of the nodal points k_P and k_E are not much different, the nodal-face conductivity k_e calculated by either the arithmetic or harmonic mean will be much the same. For the case when k_P is much different than k_E, the values of k_e calculated by Eqs (16) and (17) will be significantly different. By calculating the heat flux at a nodal face under extreme conditions of the values of thermal conductivities on either side of the interface, Patankar [26;27] showed that the use of the harmonic mean is physically more realistic than the use of the arithmetic mean.

Conclusions

A numerical model, based on the finite-volume method, was developed for the calculation of steady, two-dimensional temperature distribution in a composite slab with temperature-dependent thermal conductivity. The results of application to four cases were compared using various temperature-conductivity relations. The numerical model was validated by comparing results with possible analytical solutions; the agreement was excellent. A parametric study was conducted to investigate the effects of numerical and physical parameters on the temperature distribution. The results showed that for a conductivity ratio greater than about 100, the temperature remained unaltered to change in conductivity. For the same finite-difference grid size, more accurate results could be achieved by using the harmonic mean of nodal-face conductivity as compared to using the arithmetic mean. Future work would be directed towards the inclusion of thermal interface resistance, based on empirical data, handling of arbitrary-shape domains and extension to time-dependent temperature variation. Experimental studies are also needed in these areas since analytical solutions would cease to exist.

References

[1] Ozisik, M.N. *Heat Conduction.* New York: John Wiley, 1980.

[2] Zaki, G.M. and Hassan, K.E. "Thermal Performance of Composite Building Components with Periodic Solar Insolation and Ambient Temperature." *Solar & Wind Technology,* 3 (1986), 103-109.

[3] Shitara, T.; Matsumoto, S. and Suzuki, M. "New Numerical Method for Solving Problems Involving One-dimensional Unsteady Thermal Conduction in Laminated Binary Materials." *Int. Chem. Eng.,* 27 (1987), 76-84.

[4] Al-Mujahid, A. and Zedan, M.F. "Transient Heat Conduction Response of a Composite Plane Wall." *Warme-und Stoffubertragung,* 26 (1990), 33-39.

[5] Zedan, M.F. and Mujahid, A.M. "Laplace Transform Solution for Heat Transfer in Composite Walls with Periodic Boundary Conditions." *J. Heat Transfer*, 115 (1993), 263-265.

[6] Han, L.S. "Periodic Heat Conduction Through Composite Panels." *J. Thermophysics*, 1 (1987), 184-186.

[7] Sunden, B. "Transient Heat Conduction in a Composite Slab by a Time-varying Incident Heat Flux Combined with Convective and Radiative Cooling. *Int. Comm. Heat Mass Transfer*, 13 (1986), 515-522.

[8] Hagen, K.D. "A Solution to Unsteady Conduction in Periodically Layered, Composite Media using a perturbation Method." *J. Heat Transfer*, 109 (1987), 1021-1023.

[9] Yang, K.-T. "Transient Conduction in a Semi-infinite Solid with Variable Thermal Conductivity." *J. Appl. Mechanics*, 25 (1958), 146-147.

[10] Halle, H. "Exact Solution of Eelementary Transient Heat Conduction Problem involving Temperature-dependent Properties." *J. Heat Transfer*, 87 (1965), 420-421.

[11] Aziz, A. and Na, T.Y. Periodic Heat Transfer in Fins with Variable Thermal Parameters." *Int. J. Heat Mass Transfer*, 24 (1981), 1397-1404.

[12] Jones, Jr. O.C. "A Perturbation Method for Nonlinear, One-dimensional Conduction with Heat Generation." *Seventh Int. Heat Transfer Conference*, Munchen, 2 (1982), 9-14.

[13] Kar, A.; Chan, C.L. and Mazumder, J. "Comparative Studies on Nonlinear Hyperbolic and Parabolic Heat Conduction for Various Boundary Conditions: Analytic and Numerical Solutions." *J. Heat Transfer*, 114 (1992), 14-20.

[14] Huang, S.C. and Chang, Y.P. "Heat Conduction in Unsteady, Periodic and Steady States in laminated Composites." *J. Heat Transfer*, 102 (1980), 742-748.

[15] Palisoc, A.L.; Min, Y.J. and Lee, C.C. "Thermal Properties of Five-layer Infinite Plate Structures with Embedded Heat Sources." *J. Appl. Phys.*, 65 (1989), 4438-4444.

[16] Tamma, K.K. and Yurko, A.A. "Finite-element Thermal Modeling Analysis Formulations for Layered Composite Materials." *Numerical Heat Transfer*, Part B, 15 (1989), 73-97.

[17] Chu, H.-S.; Weng, C.-I. and Chen, C.-K. "Transient Response of a Composite Straight Fin." *J. Heat Transfer*, 105 (1983), 307-311.

[18] Ghoshdastidar, P.S. and Mukhopadhyay, A. "Transient Heat Transfer from a Straight Composite Fin: A Numerical Solution by ADI." *Int. Comm. Heat Mass Transfer*, 16 (1989), 257-265.

[19] Ju, Y.-H.; Shih, T.-P.; Chiu, C.-Y. and Lee, W.-C. "Design of a Trilaminated Rectangular Fin." *Int. J. Heat Mass Transfer*, 34 (1991), 1097-1104.

[20] Mikhailov, M.D. and Ozisik, M.N. "Transient Conduction in a Three-dimensional Composite Slab." *Int. J. Heat Mass Transfer*, 29 (1986), 340-342.

[21] Campo, A. "Estimate of the Transient Conduction of Heat in Materials with Linear Thermal Properties Based on the Solution for Constant Properties." *Warme- und Stoffubertragung*, 17 (1983), 1-9.

[22] Wrobel, L.C. "A Novel Boundary Element Formulation for Nonlinear Transient Heat Conduction." In: R.W. Lewis *et al.* (Eds) *Numerical Methods in Thermal Problems*, Vol. V, Part 2, (1987), 1348-1357.

[23] Zhao, Q.; Feddes, J.J.R. and Leonard, J.J. "A Finite Difference Model of Heat Conduction through Soil under a Barn." *Canadian Agricultural Eng.*, 31 (1989), 179-185.

[24] Chang, K.C. and Payne, U.J. "Analytical Solution for Heat Conduction in a Two-Material-Layer Slab with Linearly Temperature Dependent Conductivity." *J. Heat Transfer*, 113 (1991), 237-239.

[25] Gosman, A.D.; Launder, B.E. and Rèece, G.J. *Computer-aided Engineering Heat Transfer and Fluid Flow*. Chichester: Ellis Horwood, 1985.

[26] Patankar, S.V. "A Numerical Method for Conduction in Composite Materials, Flow in Irregular

Geometries and Conjugate Heat Transfer." *Sixth Int. Heat Transfer Conf.*, Toronto, Canada, 3 (1978), 297-302.

[27] Patankar, S.V. *Numerical Heat Transfer and Fluid Flow*. Washington: Hemisphere, 1980.

APPENDIX

Computational Details and Typical Computer Output

The calculations are carried out on a MITAC/MPC 2386 micro-computer and require about 5×10^{-4} s of CPU time per (grid node × iteration). Converged results are obtained after about 10-100 field iterations depending upon the grid size. Typical computer output using a coarse grid of NI = 8 and NJ = 6 is included in Table A1. The headings give information regarding the case considered (Case 3 in the present example), dimensions of the slab, dimensionless temperatures at the boundaries and the use of the harmonic mean of nodal-face conductivity. The thermal conductivities (k's), coefficients (β's) and exponents (n's) used in the conductivity-temperature relation [Eq. (5)] are printed next. The grid size, interface location, under-relaxation factor and convergence tolerance then follow, respectively. The interface is located in the middle of domain; for the current grid it is between nodal points I = IX1 = 4 and I = IX2 = 5. The tolerance gives a setting for the level of normalized total residual error at which the calculations are taken as converged. The solution is monitored at every iteration (ITER) by printing the sum of absolute values of nodal energy-rate imbalances (residual errors) for the whole field (ERROR) and the temperature at the monitoring point (there, I = 4 and J = 3). The value of ERROR is normalized by a typical heat transfer rate given by: $0.5\ k_1\ (T_l - T_b)\ l/\omega$. As seen in the present example, the solution stops after 11 field iterations when ERROR falls below 10^{-3} (the value set for TOLER) and the temperature at the monitoring grid point settles down to a converged value. The convergence is monotonic and fast; the errors are reduced by four orders of magnitude in 11 iterations. The field values of the temperatures obtained by the numerical and analytical solutions, and the thermal conductivity are then printed. The nodal numbers (I and J) and their corresponding coordinates (X and Y) are also printed to locate the variable values on the two-dimensional field as shown. It is interesting to note, for example, the variation of the thermal conductivity with temperature and material in the composite. Material 1 spans the grid nodes given by I = 1 to 4 and J = 1 to 6. Finally, the discrepancy between the numerical and exact solutions is due to the use of a coarse numerical grid, see Section of "Finite-difference grid independence test."

Table (A1). Typical computer output for a coarse grid

Case 3: Conduction in composite slab with linear temp.-dependent conductivity

Length	Width	T bot	T left	T right	H armonic
1.000E + 00	5.000E − 01	0.000E + 00	1.000E + 00	1.000E − 01	.True.
K1	K2	Beta 1	Beta 2	N1	N2
1.000E + 02	1.000E + 00	2.000E + 00	2.000E + 00	1.000E + 00	1.000E + 00
NI	NJ	IX1	IX2	Alpha	Toler
8	6	4	5	1.000E + 00	1.000E − 03

Iter	Error	T(4,3)
1	7.342E + 00	2.071E − 01
2	3.847E + 00	3.206E − 01
3	1.648E + 00	3.611E − 01
4	6.393E − 01	3.768E − 01
5	2.482E − 01	3.827E − 01
6	9.481E − 02	3.850E − 01
7	3.615E − 02	3.858E − 01
8	1.375E − 02	3.862E − 01
9	5.233E − 03	3.863E − 01
10	1.990E − 03	3.863E − 01
11	7.554E − 04	3.864E − 01

T (Numerical solution)

I=	1	2	3	4	5	6	7	8	Y =
J									
6	1.000E + 00	8.598E − 01	6.992E − 01	5.992E − 01	4.652E − 01	3.017E − 01	1.744E − 01	1.000E − 01	.500
5	1.000E + 00	8.553E − 01	6.926E − 01	5.922E − 01	4.593E − 01	2.976E − 01	1.725E − 01	1.000E − 01	.440
4	1.000E + 00	8.193E − 01	6.399E − 01	5.363E − 01	4.118E − 01	2.654E − 01	1.576E − 01	1.000E − 01	.320

T (Numerical solution)

I=	1	2	3	4	5	6	7	8	Y =
J									
3	1.000E + 00	6.983E − 01	4.881E − 01	3.864E − 01	2.886E − 01	1.835E − 01	1.181E − 01	1.000E − 01	.180
2	1.000E + 00	3.873E − 01	2.085E − 01	1.512E − 01	1.098E − 01	6.971E − 02	5.539E − 02	1.000E − 01	6.000E − 02
1	1.000E + 00	0.000E + 00	0.000E + 00	0.000E + 00	0.000E + 00	0.000E + 00	0.000E + 00	1.000E − 01	.000
X =	0.000	.100	.250	.410	.590	.750	.900	1.00	

T (Exact solution)

I=	1	2	3	4	5	6	7	8	Y =
J									
6	1.000E + 00	8.865E − 01	7.322E − 01	6.308E − 01	4.960E − 01	3.228E − 01	1.881E − 01	1.000E − 01	.500
5	1.000E + 00	8.837E − 01	7.264E − 01	6.238E − 01	4.899E − 01	3.186E − 01	1.862E − 01	1.000E − 01	.440
4	1.000E + 00	8.584E − 01	6.763E − 01	5.665E − 01	4.399E − 01	2.844E − 01	1.701E − 01	1.000E − 01	.320
3	1.000E + 00	7.654E − 01	5.250E − 01	4.127E − 01	3.116E − 01	1.982E − 01	1.287E − 01	1.000E − 01	.180
2	1.000E + 00	4.685E − 01	2.447E − 01	1.771E − 01	1.280E − 01	7.851E − 02	5.919E − 02	1.000E − 01	6.000E − 02
1	1.000E + 00	0.000E + 00	0.000E + 00	0.000E + 00	0.000E + 00	0.000E + 00	0.000E + 00	1.000E − 01	.000
I =	0.000	.100	.250	.410	.590	.750	.900	1.00	

Thermal conductivity

I=	1	2	3	4	5	6	7	8	Y =
J									
6	3.000E + 02	2.720E + 02	2.398E + 02	2.198E + 02	1.930E + 00	1.603E + 00	1.349E + 00	1.200E + 00	.500
5	3.000E + 02	2.711E + 02	2.385E + 02	2.184E + 02	1.919E + 00	1.595E + 00	1.345E + 00	1.200E + 00	.440
4	3.000E + 02	2.639E + 02	2.280E + 02	2.073E + 02	1.824E + 00	1.531E + 00	1.315E + 00	1.200E + 00	.320
3	3.000E + 02	2.397E + 02	1.976E + 02	1.773E + 02	1.577E + 00	1.367E + 00	1.236E + 00	1.200E + 00	.180
2	3.000E + 02	1.775E + 02	1.417E + 02	1.302E + 02	1.220E + 00	1.139E + 00	1.111E + 00	1.200E + 00	6.000E − 02
1	3.000E + 02	1.000E + 02	1.000E + 02	1.000E + 02	1.000E + 00	1.000E + 00	1.000E + 00	1.200E + 00	.000
X =	.000	.100	.250	.410	.590	.750	.900	1.00	
00									